In situ hydrothermal crystallization of hexagonal hydroxyapatite tubes from yttrium ion-doped hydroxyapatite by the Kirkendall effect

CrossMark

Chengfeng Li [a,*], Xiaolu Ge [b], Guochang Li [a], Hao Lu [a], Rui Ding [a]

[a] School of Materials Science and Engineering, Shandong University of Technology, 255049 Shandong, PR China
[b] School of Science, Shandong University of Technology, 255049 Shandong, PR China

ABSTRACT

An in situ hydrothermal crystallization method with presence of glutamic acid, urea and yttrium ions was employed to fabricate hexagonal hydroxyapatite (HAp, $Ca_5(PO_4)_3(OH)$) tubes with length of 200 nm–1 μm. Firstly, yttrium ion-doped HAp (Y-HAp, $Ca_{5-x}Y_x(PO_4)_3(OH)$) was synthesized after hydrolysis of urea and HPO_4^{2-} ions at 100 °C with a dwell time of 24 h. The shift of X-ray diffraction peaks of HAp to high angle was caused the substitution of Ca^{2+} ions by small-sized Y^{3+} ions. At 160 °C, further hydrolysis reactions of urea and HPO_4^{2-} ions resulted in the generation of ample OH^- and PO_4^{3-} ions, which provided a high chemical potential for the dissolution of Y-HAp and recrystallization of HAp and YPO_4. Finally, HAp tubes were formed in situ on Y-HAp according to the Kirkendall effect as a result of the difference of diffusion rate of cations (Ca^{2+} ions, outward and slow) and anions (OH^- and PO_4^{2-} ions, inward and fast). The formation process of HAp tube was simulated by the encapsulation of fluorescein molecules in precipitates. Photoluminescence properties were enhanced for HAp tubes with thick and dense walls. This novel tubular material could find wide applications as carriers of drugs, dyes and catalysts.

© 2014 Elsevier B.V. All rights reserved.

1. Introduction

Hollow nanoparticles have received considerable attention due to their great promise in multiple applications as support for catalysts, drugs and dyes [1,2]. Many versatile fabrication methods are developed to synthesize hollow crystals through either the Kirkendall effect or the Ostwald ripening [2–4]. Synthetic hydroxyapatite (HAp, $Ca_5(PO_4)_3(OH)$) is similar to inorganic constitute of human bones and teeth. The bioactivity, biocompatibility and stability properties of HAp are determined by their morphology, size, composition and structure [5,6]. Numerous reports have been focused on the morphological control of HAp for fabrication of rod (or fiber)-like [7,8] and plate-like [9] shapes. The morphological evolution could provide scientific significance and practical applications, such as simulation of unfavorable growth of bones and encapsulation of proteins and drugs. However, the loading capacity is not optimal because of lack of macro/nanopores or hollow interiors in crystals. Furthermore, some problems related to the release behavior of molecules from these materials have not been solved, such as initial burst release and short-term release [10].

Although many efforts have been devoted, synthesis of hollow rod-like HAp with designed chemical components and controlled crystal morphologies is rarely reported [11]. Polycrystalline microtubes were obtained using template materials of glass [10], dibasic calcium phosphate ($CaHPO_4$) nanorods [11], cotton [12] and calcium oleate precursor [13]. Ma et al. [14] developed a simple solvothermal method to produce HAp microtubes in a mixed solvent of water/N,N-dimethylformamide. However, N,N-dimethylformamide is harmful for the human health and the environment (soil, air and water). The preparation of tubular rod with a well-defined shape becomes a great challenge before the clarification of formation mechanism of hollow HAp. Herein, we demonstrate a facile in situ hydrothermal crystallization method to fabricate hollow HAp with sharp hexagonal shape and varied lengths through the Kirkendall effect.

2. Experimental

2.1. Synthesis of sample

Products of calcium phosphate were prepared by a modified in situ hydrothermal crystallization method as reported in [15,16]. Chemical reagents with analytical purity were added to 45 ml of aqueous solution with the following sequence: 0.60 g of L-glutamic acid, 0.38 g of sodium phosphate dibasic dodecahydrate ($Na_2HPO_4 \cdot 12H_2O$), 0.07 g of sodium hydroxide (NaOH), 0–3.0 ml of aqueous yttrium nitrate solution ($Y(NO_3)_3$, 0.2 mol/l), 0.15 g of urea and 0.14–0.28 g of calcium nitrate tetrahydrate ($Ca(NO_3)_2 \cdot 4H_2O$). The total amount of Ca^{2+} and Y^{3+} ions was kept constant at 1.18 mmol. For example, when 1.0 ml of $Y(NO_3)_3$ solution was added, reaction solution was finally prepared with the presence of 0.23 g of calcium nitrate tetrahydrate. After

addition of 0.02 g of fluorescein, the mixture was sealed in a 50 ml Teflon container and then raised to 100 °C. After 24 h, the hydrothermal treatment was performed at 160 °C for 0–24 h. As-received precipitates were obtained after separation and finally dried at 60 °C for 24 h. The denotation of sample, for example, S15-24 was according to the addition of 1.5 ml of $Y(NO_3)_3$ solution and the hydrothermal treatment performed at 160 °C for 24 h. The sample was also synthesized with the absence of fluorescein through the above-mentioned procedure and denoted as S15-24-0Flu.

2.2. Characterization

Samples were characterized by X-ray diffraction (XRD) on a D8 advanced X-ray diffractometer (Cu-k_α radiation, wavelength: $\lambda = 0.15406$ nm). The crystal morphologies were characterized by scanning electron microscopy (SEM, FEI SIRION 200). Energy dispersive X-ray (EDX) spectroscopy (INCA energy 350, OXFORD, UK) was used to analyze the composition. Fourier transform infrared (FTIR, Nicolet 5700, Thermo, USA) spectra were obtained with the wavenumbers recorded from 400 to 4000 cm^{-1} at a 1 cm^{-1} resolution.

3. Results and discussion

3.1. XRD characterization

With absence of Y^{3+} ions in reaction solutions, S0-0, S0-12 and S0-24 were synthesized and identified by XRD as shown in Fig. 1. When hydrothermal treatment was performed at 160 °C for a prolonged time, octacalcium phosphate (OCP, JCPDS No. 26-1056) for S0-0 was converted to HAp (JCPDS No. 09-0432) for S0-12 and S0-24, which was similar with our previous report [16]. Yttrium dopants enhanced osteoblast adhesion and calcium deposition onto HAp coatings, indicating that yttrium ion-dopped HAp (Y-HAp, $Ca_{5-x}Y_x(PO_4)_3(OH)$) might improve the performance of orthopedic and dental implants [17,18]. Herein, Y-HAp was synthesized through a hydrothermal route with different additions of yttrium ions. As shown by XRD characterization in Fig. 2(a) and (b), S15-0 and S15-12 were identified as purity phases of HAp. Relative to those of standard HAp and bare HAp of S0-24 (Fig. 1(c)), the diffraction peaks of S15-0 and S15-12 became broad and shifted to high angle because of the substitution of the Ca^{2+} ion (1.00 Å) with the smaller Y^{3+} ion (0.90 Å) [19]. When the hydrothermal treatment was performed at 160 °C for 12 h, crystallite intensities of S15-12 increased obviously. After 24 h, both HAp and YPO_4 (JCPDS No. 84-0335) phase were observed, indicating the occurrence of the dissolution of Y-HAp and recrystallization of HAp and YPO_4. When more
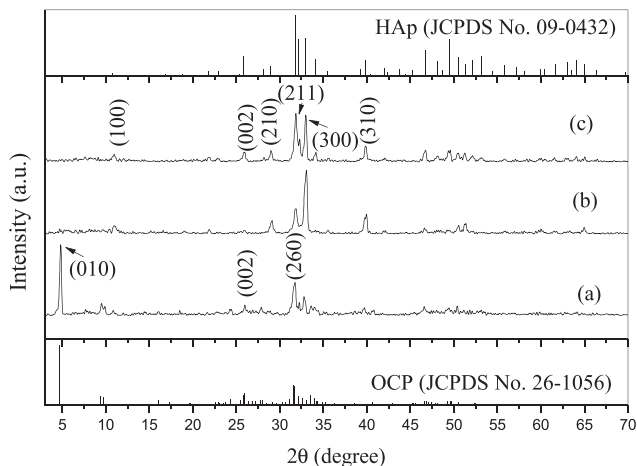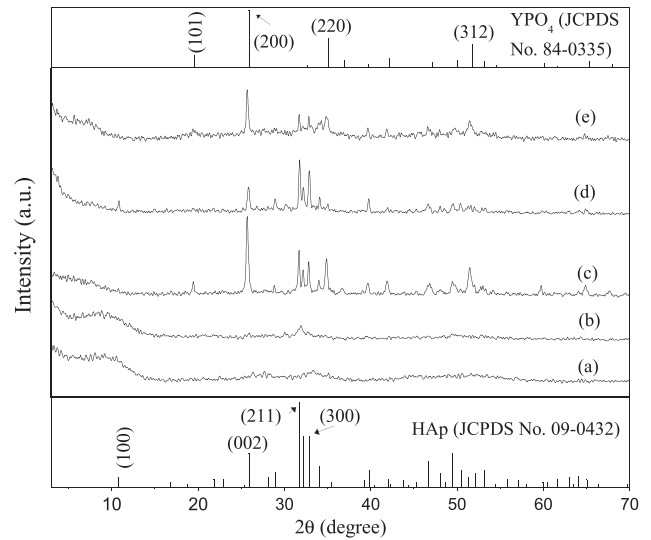

Fig. 2. XRD patterns of S15-0 (a), S15-12 (b), S15-24 (c), S10-24 (d) and S30-24 (e).

Y^{3+} ions were added, YPO_4 became more prominent as shown in Fig. 2(d), (c) and (e). According to the diffraction peak of HAp's (300) plane, crystallite sizes for S10-24, S15-24 and S30-24 were calculated by the Scherrer's equation as 35, 74 and 80 nm, respectively.

3.2. SEM characterization

Without addition of Y^{3+} ions, micro-sized HAp whiskers of S0-24 were synthesized as shown in Fig. 3 (a and b), which was similar with previous studies [15,20–25]. With the presence of Y^{3+} ions, the crystallization of HAp occurred quite differently during hydrothermal treatment. SEM characterization was used to monitor the morphological variation of samples with reaction time and addition of Y^{3+} ions as shown in Fig. 3(b)–(h). Spherical nanoparticles of S15-0 possessed a fine and relatively uniform structure. For S15-12, rod-like particles appeared and some of them became hollow. Although the amount of spherical particles decreased, the variation of their morphology was hardly observed. After hydrothermal treatment performed at 160 °C for 24 h, spherical particles disappeared almost completely and hexagonal tubes of S15-24 with a length of about 200 nm were fabricated, which indicated the occurrence of a dissolution and in situ recrystallization process. When increasing the addition of Y^{3+} ions, the lengths of tubes increased as shown in Fig. 3(f), (e), (g) and (h). For S30-24, the length of HAp tubes became almost 1 μm and small YPO_4 particles were also observed with sizes of 100–200 nm. With addition of more Y^{3+} ions, concentration of Ca^{2+} ions in Y-HAp decreased and then less Ca^{2+} ions were released into reaction solutions after the dissolution of Y-HAp, which resulted in the reduction of the supersaturation degree of HAp. Nucleation rate of HAp during crystallization in reaction solution decreased and large-sized HAp tubes were synthesized. When the ratio of (Ca + Y)/P was raised to 5:3 (1.67) through increasing the addition of Ca^{2+} ions, the sample of S15-24-167 was synthesized and the formation of HAp tube was not observed as shown in Fig. 3(i).

3.3. FTIR spectra

The chemical compositions of crystals were evaluated more specially using FTIR spectra as shown in Fig. 4. All characteristic absorbance bands of HAp were observed, such as for S0-24-0Flu (Fig. 4(a)), including bands assigned to PO_4^{3-} (564.2, 602.6, 1034.3 and 1095.0 cm^{-1}) and OH^- (located at 3568.7 cm^{-1}) [26]. The broad band from 3650 to 3000 cm^{-1} was due to the water molecules present on the synthesized substance. The adsorption bands located at 2858.0 and 2929.4 cm^{-1}

Fig. 1. XRD patterns of S0-0 (a), S0-12 (b) and S0-24 (c).